ADVANCES IN TRANSPORTATION STUDIES
An International Journal

Editor in Chief: Alessandro Calvi

Vol. LXVI July 2025

Contents

aracne

Advances in Transportation Studies: an international Journal 66 (2025)

ISBN 979-12-218-1935-9 – ISSN 1824-5463 – DOI 10.53136/97912218193591 – pag. 3-18

The joint signal timing and route choice on networks considering increment

T. Xu S. Fan A. Cheng L. Zhang X. Shu

School of Civil and Transportation Engineering at Henan University of Urban Construction, China
email: selecxtz@126.com

subm. 30th September 2024 *approv. after rev. 12nd November 2024*

Abstract

Selecting the length of the increment is important in solving the optimal signal timing (OST) and the dynamic user optimal route choice (DUORC) problem. How large should the increment in the solution process be? The study of this problem is rare. In this paper, the OST and the DUORC problem was studied with the consideration of assignment increment. The problem is modeled as a three-level problem and the experimental study is done. The first level is setting the increment. The second level minimizes total travel time. The third level is a variational inequality (VI) DUORC model. The result of the experimental study shows that a smaller increment can increase the precision of the solution. Since the signal cycle at an intersection cannot be less than the minimum cycle, the study indicates that a small increment is preferred in solving the OST-DUORC problem as long as the minimum green time is reached. Furthermore, this paper presents a conception of a new OST-DUORC travel guidance system, including the framework of the system and the algorithm for it. With the method, the traffic center selects an appropriate increment based on the result of this study, and then finds the OST for intersections and the optimal routes for travelers by running the second and third level model. The method helps implement a transport system integrated with a traffic control system and a DUORC guidance system.

Keywords – dynamic user optimal, increment, route choice, signal timing, transportation network

1. Introduction

In a transport system integrated with a traffic control system and a dynamic user optimal route choice (DUORC) guidance system, a transport management center of a city sends the optimal routes to travelers before they start their journeys and sets the optimal signal setting for all the signalized intersections. In this way, the overall travel cost of all travelers is minimal and meanwhile, the route choice of all travelers is in dynamic user optimal (DUO) status. To do this, the transport management center must solve the optimal signal timing (OST) and DUORC problem (OST-DUORC). The OST-DUORC is often modeled as a bi-level problem with the upper level problem being OST and the lower level problem being dynamic traffic assignment (DTA) following either user-optimal [1-4] or system-optimal [5, 6]. The algorithms used in past studies include reactive tabu search (RTS), genetic algorithms [4, 7], simulation-based method [1, 2], relaxation with gradient projection algorithm [8], etc.

Past related studies include signal control on static transportation networks [9-22], a combination of signal timing and DTA [1, 2, 7, 18, 20], combined optimization problem [12], adaptive signal control [23], dynamically adjusting offsets [24], lane-based signals [25], dynamic signal timing with dilemma-zone protection [26], adaptive signal processing [27], optimization and

coordination of signal control [28], dynamic predictive traffic signal control [29], adaptive signal control [30], traffic signal optimization [31], dynamic nature of dilemma zone [32], dynamic lane-use assignment [33], dynamic eco-driving near signalized intersections [34], dynamic speed strategy [35], estimate queue length [36], dynamic reversible lanes [37], the delay of right-turning vehicles [38], dual-target dynamic optimization [39], delay models [40-52], etc. Since none of these studies are about the DUO problems on the multiple origins multiple destinations (MOMD) dynamic transportation networks, they do not apply to the OST-DUORC problem in this study.

In this study, the method in [8] is adopted for the OST-DUORC problem. However, in modeling and solving the OST-DUORC problem by the method in [8], an increment is always needed to discretize the study period (actually for any method in solving the DUORC problem, the selection of the increment is a must issue). The flow propagation on a link at different iterations is always fixed with a given number of increments at the iteration. The length of the increment selected in the solution process ranged from 10 seconds in some models (such as the cell transmission model) to five minutes or more in other methods. The length of the increment is critical in deciding the level of the precision of the solution. By variating the increment, the solution of the DUORC at different granularity can be obtained. From the theoretical point of view, the smaller the increment is, the smaller the error in estimating the travel time of links or paths, and vice versa. For the variational inequality (VI) model, the error is due to the round-off of link travel times used in the link flow propagation at each relaxation of the lower VI DUORC problem. For the DUORC problem on a signalized transportation network, a smaller increment also means a smaller error in signal timing [8]. However, the green time cannot be too small and the minimum green time for a phase at a signalized intersection must be considered in reality. How large should the increment in the solution process be set considering both the precision of the solution and the practice of signal timing? The experimental study of this problem is rare.

In this study, we presented a three-level model for the joint signal timing and route choice on networks considering increment for the experimental study of the problem. Furthermore, this paper presents the conception of a new OST-DUORC travel guidance system. Based on the literature review of this study, the new OST-DUORC travel guidance system has not been studied yet so far. With the method presented in this paper, the traffic center selects an appropriate increment based on the experimental result of this study and then finds the OST for intersections and the optimal routes for travelers by running the second and third level model.

The remaining of the paper is arranged as follows: Section 2 introduces a three-level model for the experimental study. Section 3 presents a solution method for the three-level model. Section 4 shows the validity of the model and the algorithm by applying them to a simulation network and doing the experiment. Section 5 presents the conclusion of the paper.

2. OST-DUORC model

In this section, the OST-DUORC problem with the consideration of increment is formulated as a three-level model. The first level is setting the increment. The second and the third level combined are a non-cooperative Stackelberg game. In the game, the transport management center is the leader of the game and sets signal timing to minimize overall queuing delay. The travelers in the calculation are the followers of the game who select their routes as a reaction to signal timing to minimize their costs. The interplay between the transport management center and travelers finally reaches an equilibrium in which traffic signal timing reaches optimal and travelers choose user-optimal routes. This is done by the calculation conducted by the transport management center in the OST-DUORC environment.

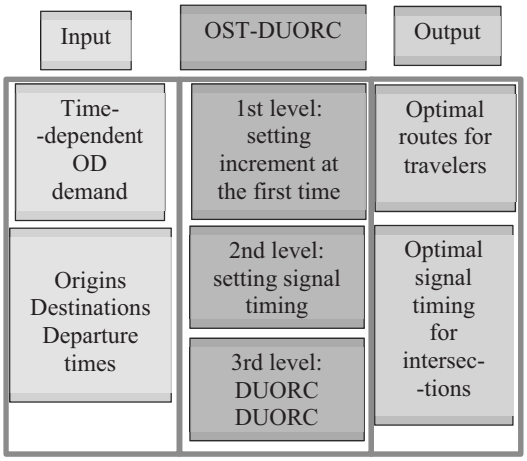

Fig. 1 - The illustration of the three-level model

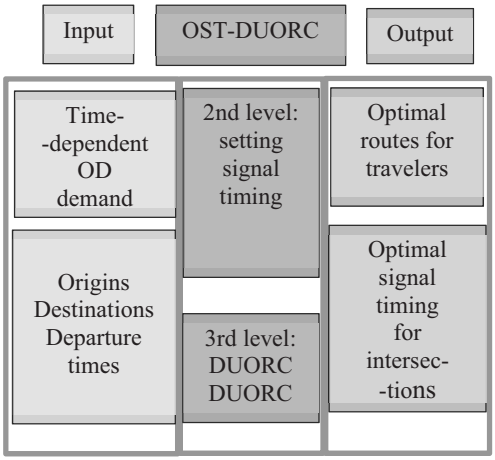

Fig. 2 - The illustration of the integrated OST-DUORC model

The illustration of the integrated OST-DUORC model with the consideration of increment is shown in Fig. 1. The illustration of the integrated OST-DUORC model given the increment is shown in Fig. 2. It should be noted that selecting an appropriate increment by running the three-level model only needs to be done in this paper based on Fig. 1. For the transport center, they only need to find the OST for intersections and the optimal routes for travelers by running the second and third level model based on Fig. 2. Based on the result of this study, they should select a smaller increment possible considering the minimum cycle in their signal control systems, as will be covered in the next section.

The input is the time-dependent origin destination (OD) demand. In the OST-DUORC environment, the travelers send their origins, destinations, and departure times to the transport management center by simply clicking the origins and destinations of their journey and entering the desired departure times on the electronic map of the user terminal of the online travel guidance system. After aggregating all the individual data, the time-dependent OD demand for each OD is obtained. The OST-DUORC solver solves the OST-DUORC problem and finds the optimal routes for travelers and the optimal signal timing for intersections. The optimal routes are shown to travelers on their electronic maps and the optimal signal timing is set for intersections. The difference between the optimal routes provided by the integrated OST-DUORC from the optimal routes in today's maps lies in that not only the links/streets and nodes/intersection will be shown, but the signal timing at each intersection and the traversing time on each street on the route will also be shown. What's more, the overall queuing delay of all vehicles at intersections is minimal and meanwhile, the route choice of all travelers is in DUO status.

The relevant notations for variables are defined as follows. $[0, T_0]$: departure horizon or the period when vehicles are departing from an origin and entering the network. $[0, T]$: the period from the beginning to the time point at which the last vehicle entering the network reaches its destination. x_a^k: the number of vehicles on link a at beginning of interval k. u_a^k: inflow into link a during interval k. v_a^k: exit flow from link a during interval k. S_a: the saturation flow rate for link a. q_a^k: the total number of vehicles queued at or entering the exit of link a at k. $q_a^{k,r}$: the number of vehicles queued

at the exit of link a in red time increment k. $q_a^{k,g}$: the number of vehicles joining the queue at the exit of link a or entering the intersection during the green time increment k. $u_a^{rs}(k)$: inflow into link a from origin r to destination s at time k. $v_{a,k}^{rs}$: outflow from link a from origin r to destination s at time k. f_k^{rs}: departure flow from origin r toward destination s during interval k. $\tau_a^k(\cdot)$: actual travel time over link a for flows entering link a at time k. $\tau_a(0)$: the travel cost on link a when there is no queue at the downstream of the link. $\bar{\tau}_a(0)$ is the rounded integer of $\tau_a(0)$. $f_{p,k}^{rs}$: flow for route p between origin r and destination s during interval k. $\eta_{p,k}^{rs}$: actual travel time for route p between OD pair rs for flows departing origin r at time k. $\eta_{p,k}^{ri}$: actual travel time for route p between origin r and node i for flows departing origin r at time k. In this paper, when the superscript is too long, it can also be put into a pair of square parenthesis after the variable.

Without loss of generality, a phase only consists of effective red time and effective green time. Define a link's cycle as the cycle of the link's downstream intersection. For the reason of first-in-first-out (FIFO) respect and accuracy [52], the following point-queue (PQ) model is adopted to estimate the link travel time.

$$\tau_a^k(\cdot) = \begin{cases} \tau_a(0) + q_a^{(k+\bar{\tau}_a(0))}/S_a, & \left(k+\bar{\tau}_a(0)\right) \in green \\ \tau_a(0) + t_a^{k,r} + q_a^{(k+\bar{\tau}_a(0))}/S_a, & \left(k+\bar{\tau}_a(0)\right) \in red \end{cases} \tag{1}$$

where $\tau_a(0)$ is the travel cost when the link is empty. $\bar{\tau}_a(0)$ is the rounded integer of $\tau_a(0)$, $q_a\left(k+\bar{\tau}_a(0)\right)$ is the overall vehicles queued at the downstream of link a at $\left(k+\bar{\tau}_a(0)\right)$.

When traffic is not congested, we have

$$q_a^{(k+\bar{\tau}_a(0))} = \begin{cases} q_a^{(k+\bar{\tau}_a(0)-1),r} + q_a^{(k+\bar{\tau}_a(0)),g} & \left(k+\bar{\tau}_a(0)\right) \in green \\ q_a^{(k+\bar{\tau}_a(0)),r} & \left(k+\bar{\tau}_a(0)\right) \in red \end{cases} \tag{2}$$

The three-level model is defined as follows.

The first level is setting the increment Δt. Abbreviate Δt as Δ. The first level is selecting Δ to

$$\min_{g_{min}<\Delta<\epsilon_{max}} Z_1 = Z_2 + Z_3 \tag{3}$$

where g_{min} is the minimum green time of a phase in reality, and ϵ_{max} is the maximum of the allowable round-off error in link travel times used in the link flow propagation at each relaxation of the VI DUORC problem. Z_2 and Z_3 are the objective function value for the second level and the third level of the model, respectively.

The second level of the model is defined as

$$\min_{\mathbf{g},\mathbf{r}} Z_2 = \sum_k \sum_a u_a^k \tau_a^k(\cdot) \tag{4}$$

where **g** and **r** are the green time and red time. (4) is the total travel time spent by all the travelers in completing their journey, which follows the SO principle.

The third level of the model is defined as the following discrete VI DUORC model including (5) - (15).

$$\sum_{r,s,p} \sum_{k=1}^{K_0} \eta_{p,k}^{rs*} \left(f_{p,k}^{rs} - f_{p,k}^{rs*}\right) \geq 0 \tag{5}$$

where * means the path flow and path time is estimated at the optimal status, and $\boldsymbol{\eta}, \mathbf{f} \in \boldsymbol{\mathcal{R}}_+^{|P|\times K_0}$,

$$\eta_{p,k}^{ri} = \eta_{p,k}^{r(i-1)} + \tau_a\left[k + \eta_{p,k}^{r(i-1)}\right] \ \forall\, p, r, i; i = 1, 2, \cdots, s \tag{6}$$

where $p = (r, \cdots, s)$, $x \in \Theta$,. Θ is the feasible region defined by the following constraints:

Path flow conservation constraint:

$$\sum_p f_{p,k}^{rs} = f_k^{rs} \quad \forall\, k, r, s \tag{7}$$

Link inflow conservation constraint:

$$\sum_{rs} u_{a,k}^{rs} = u_a^k \quad \forall\, a,k,r,s \tag{8}$$

Link outflow conservation constraint:

$$\sum_{rs} v_{a,k}^{rs} = v_a^k \quad \forall\, a,k,r,s \tag{9}$$

Node flow conservation constraint:

$$\sum_{a\in B(j)} v_{a,k}^{rs} = \sum_{a\in A(j)} u_{a,k}^{rs}\ \forall\, j \neq r,s;\ k,r,s \tag{10}$$

where $A(j)$ is the set of links after j and $B(j)$ is the set of links before j.

Link flow propagation constraint:

$$u_{a,k}^{rs} = v_a^{rs}[k + \tau_a^k] \forall\, a,k,r,s \tag{11}$$

Inflow and queue equation

$$u_a^k = \begin{cases} q_a^{(k+\bar{\tau}_a(0)),g} & \left(k+\bar{\tau}_a(0)\right) \in green \\ q_a^{(k+\bar{\tau}_a(0)),r} & \left(k+\bar{\tau}_a(0)\right) \in red \end{cases} \tag{12}$$

Outflow and queue equation

$$v_a^{(k+\bar{\tau}_a(0))} = \begin{cases} q_a^{(k+\bar{\tau}_a(0)-1),r} + q_a^{(k+\bar{\tau}_a(0)),g} & \left(k+\bar{\tau}_a(0)\right) \in green \\ 0 & \left(k+\bar{\tau}_a(0)\right) \in red \end{cases} \tag{13}$$

Path-link flow incidence constraint:

$$u_a^{rs}(n) = \sum_{r,s,p} \sum_{k=1}^{K_0} f_{p,k}^{rs}\, \delta_{rsa}^{pkn}\ \forall\, a,k,n,\ r,s \tag{14}$$

where δ_{rsa}^{pkn} =1 if travelers departing origin r at interval k heading for destination s on path p arrives at link a during the nth interval; =0, otherwise.

Nonnegative constraint:

$$f_{p,k}^{rs} \geq 0,\ u_{a,k}^{rs} \geq 0 \quad \forall\, k,r,s,a,p \tag{15}$$

The VI DUORC model is equivalent to the following optimization problem under relaxation

$$\min_{f} Z_3 = \sum_{n=1}^{n=K} \sum_a \left\{ \int_0^{\sum_{rs} \sum_{k=1}^{K_0} \sum_p f_p^{rs}[n-\eta_p^{ri}(k)]\delta_{rsa}^{pkn}} \tau_a^k(\omega)\, d\omega \right\} \tag{16}$$

So the third level of the model under relaxation is (6) - (16).

The second level and the third level combined are a non-cooperative Stackelberg game.

3. Algorithm

The procedure of the algorithm for solving the three-level model is introduced in this section.

In the first level of the model, the increment Δ is gradually increased within the range $g_{min} < \Delta < \epsilon_{max}$. Considering the effective green time and the effective red time is used in this study, we set g_{min}=10 seconds, and the Δ is increased by 1 seconds at each iteration in the first-level model in the solution process. The ϵ_{max} is set as 60 seconds, meaning the round-off error in link travel times used in the link flow propagation at each relaxation of the VI DUORC problem is within 60 seconds. Both g_{min} and ϵ_{max} can be set as other values depending on the requirement of precision in solving the problem.

In the second level of the model, the green time and red time **g** and **r** must be set to minimize $Z_2 = \sum_k \sum_a u_a^k \tau_a^k(\cdot)$. Since the second level of the model is bounded by the solution of the third level model, **u** and **q** are given. Thus, the minimum of Z_2 is equivalent to minimizing the total queuing delay at red time of each cycle for every single signalized intersection. Based on Xu et al. [8], the latter can be minimized by assigning green time to the approach with maximal ratio, or updating the $t_a^r(k)$ based on the formula

$$t_a^{k,r(new)} = \begin{cases} green\ if\ \max\limits_{\bar{a}\in\bar{A}}\left\{\frac{\mu}{c}(\bar{a},k)\right\} > \max\limits_{\bar{\bar{a}}\in\bar{\bar{A}}}\left\{\frac{\mu}{c}(\bar{\bar{a}},k)\right\} \\ red \qquad\qquad otherwise \end{cases}, \forall\ \bar{a}\in\bar{A},\ \bar{\bar{a}}\in\bar{\bar{A}} \tag{17}$$

where $\bar{A}$ is the leg set of the intersection with the same phase as a, $\bar{\bar{A}}$ is the leg set of the intersection with conflicting phase with a, $\frac{\mu}{c}(a,k)$ is the volume/ saturation ratio of approach a (link a) of the intersection of which link a is a leg, etc. It is noticeable that if a phase is set as green its conflicting phase must be updated as red to avoid flow conflict in intersections.

In the third level of the model, the relaxation with gradient projection algorithm for solving the DUORC problem on a signalized transportation network [8] is used in this study.

The flowchart for solving the three-level model illustrated in Fig. 1 is shown in Fig. 3.

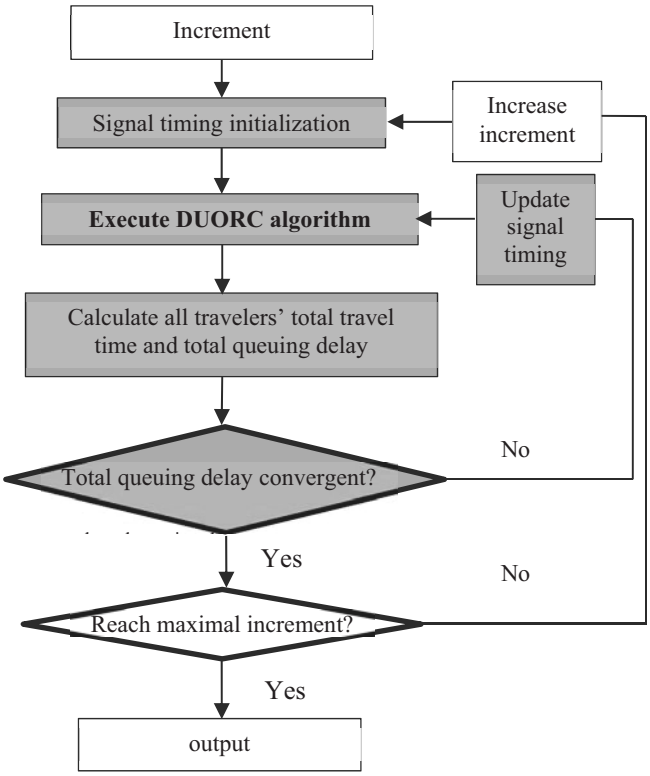

Fig. 3 - The flowchart of the algorithm

It should be noted that the part of the flowchart highlighted in light green is for solving the integrated OST-DUORC model illustrated in Fig. 2.

4. Numerical example

4.1. The simulation network

An example is introduced below to show the three-level model and algorithm. The network is shown in Fig. 4. In the network, each link stands for a 1.5-mile-long two-lane street. Links belonging to un-signalized intersections include links 24, 21, 19, 15, 10, 6, 4, and 1. All the other

links belong to signalized intersections. The phases for them are shown in Fig. 5. There are two phases in each cycle for all the signalized intersections. The cycle length is not fixed. A phase consists of effective red time and effective green time. Both the red time and green time of a phase are a multiple of the increment. The optimal signal timing is to be found by solving the OST-DUORC problem. The saturation flow rate for all links is 1 vehicle unit/second/lane. The free flow speed is 36.67 feet/second or 25 miles/hour. The links belonging to un-signalized intersections have constant link travel time $\tau_a^k = L_a/s_f + 0.35\Delta$, where L_a and s_f are the length of link a and the free flow speed, Δ is time increment. (1) is used to estimate the link travel time on other links, where $\tau_a(0) = L_a/s_f$. Four OD pairs are considered. They are 1-9, 9-1, 3-7, and 7-3. Two cases are considered. In case one, the departure period is from 7: 00 to 7: 20 AM. For OD 1-9 and 9-1, the departing flow rate is 30 vehicles/ minute from 7: 00 to 7: 05 AM. and from 7: 15 to 7: 20 AM. The departing flow rate is 40 vehicles/ minute from 7: 05 to 7: 15 AM. For OD 3-7 and 7-3, the departing flow rate is 35 vehicles/ minute from 7: 00 to 7: 05 AM. and from 7: 15 to 7: 20 AM. The departing flow rate is 50 vehicles/ minute from 7: 05 to 7: 15 AM. Case one is for the demonstration of the effect of the length of the increment. To illustrate the whole process of the OST-DUORC problem in detail, a short departure period is needed, which is the case in case two. In case two, there are five 30-second departure intervals. The time-dependent OD demand at each interval is 10 vehicles.

4.2. The effect of the increment in OST-DUORC solution

The algorithm shown in Fig. 3 was adopted to solve the three-level model in case one of the example. By variating increments and solving the Stackelberg game accordingly, the total travel cost of all vehicles, the total queue*stop in red time, and the total cost of all vehicles versus increment were found and were shown in Fig. 6, Fig. 7, and Fig. 8, respectively.

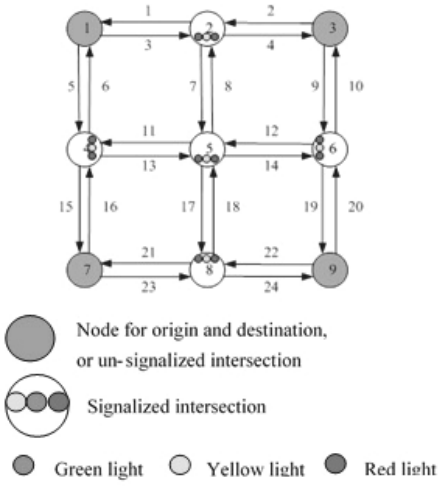

Fig. 4 - Simulation network

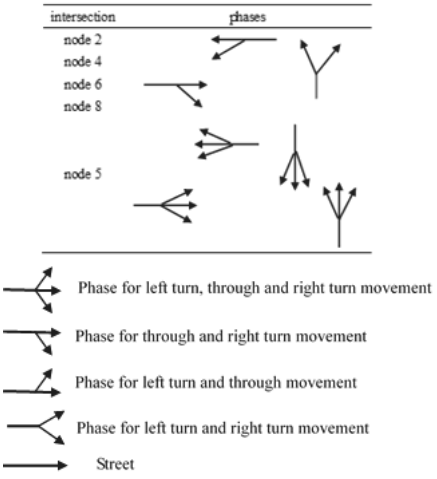

Fig. 5 - The phases for the signalized intersections

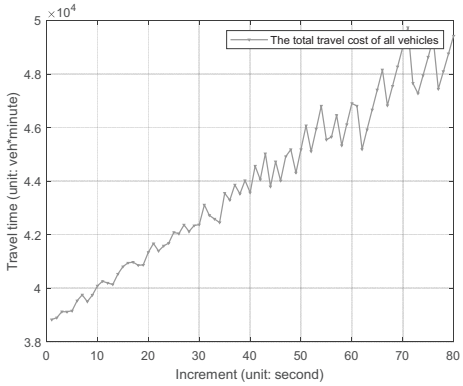

Fig. 6 - The total travel cost of all vehicles versus increment

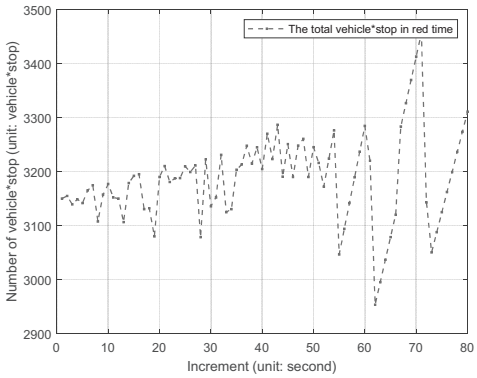

Fig. 7 - The total queue*stop in red time versus increment

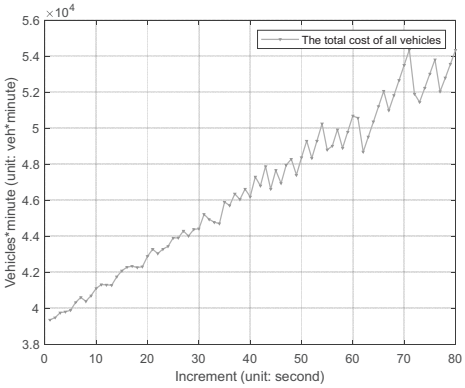

Fig. 8 - The total cost of all vehicles versus increment

The total cost of all vehicles is the sum of the total travel cost of all vehicles and the total queuing delay in red time. As can be seen in the figures, generally all of them increased with the increased increment. It can also be seen in the figures that the variation of the total travel cost of all vehicles,

the total queue*stop in red time, and the total cost of all vehicles increase with the increased increment. The increasing of cost comes from the truncation error in the solving process of the Stackelberg game. Based on the experimental study in this study, a smaller increment is preferred in solving the OST-DUORC problem to increase the precision of the solution. However, the signal cycle at an intersection cannot be less than the minimum cycle. This indicates a smaller increment is preferred as long as the minimum green time is reached. Considering the practice in reality, we set the increment as 30 seconds in the following study. The increment equalling the length of the minimum green time can be the reference in practice.

4.3. The optimal signal timing with DUO solution

Based on the result in section B, we set the increment as 30 seconds for both case one and case two. The algorithm shown in Fig. 3 (the part highlighted in light green) was adopted to solve the Stackelberg model (the second and the third level) in case one and case two of the example when the increment is set 30 seconds. After a few outer iterations, the algorithm converges with a criterion of 0.0001 of the difference of the total queued vehicles between successive iterations. The queue versus iteration for case one is shown in Fig. 9.

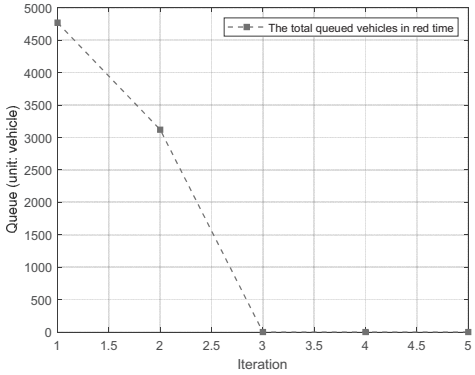

Fig. 9 - The queue versus iteration

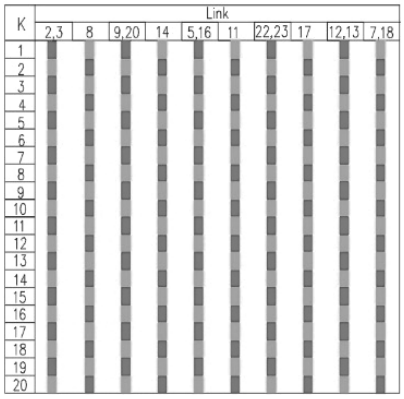

Fig. 10 - Initial signal timing
(K is an interval)

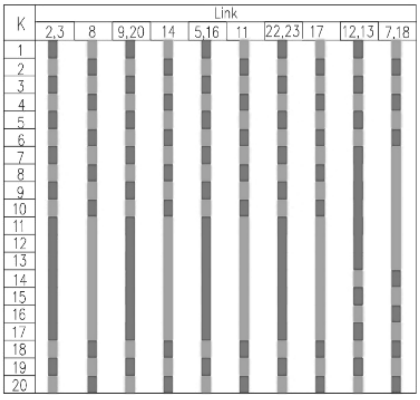

Fig. 11 - Optimal signal timing
(K is an interval)

Since the departure period and intervals in case one are far more than in case two, we only show the result for case two in the following part of the paper for conciseness. Even for case two, only part of the result is shown in this paper because of the space of the paper. But the result is similar for all the cases.

The initial signal timing for case two is shown in Fig. 10. The optimal signal setting for case two is found and is shown in Fig. 11. A careful comparison of the above figures between initial signal timing and optimal signal timing found they are very different.

Randomly taking OD 7-3 as an example, the flow on each used path under initial signal timing and optimal signal timing are shown in Fig. 12. The travel cost for each used path under initial signal timing and optimal signal timing are shown in Fig. 13. There are 13 paths used by travelers/ vehicles (with non-zero flow) under initial signal timing whereas there are 10 paths used by travelers/ vehicles under optimal signal timing. It can be seen in Fig. 13 that travelers/ vehicles from the same OD at the same departure time have equal path travel time.

Randomly taking link 23 as an example, the queued vehicles over red time and throughput over green time at link 23 under initial signal timing and optimal signal timing are shown in Fig. 14. It can be seen in the figure the number of the queued vehicles is decreased in optimal signal timing.

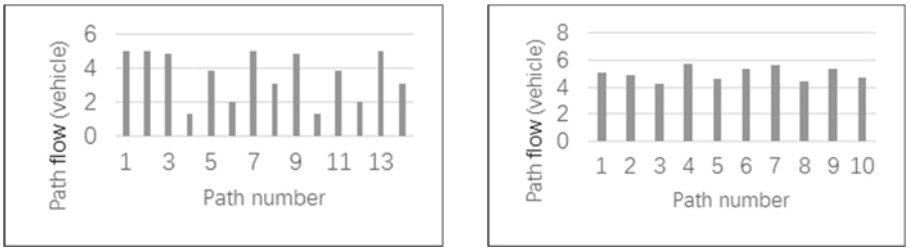

(a) (b)

Fig. 12 - The flow on each used path (OD:7-3).
(a) under initial signal timing. (b) under optimal signal timing

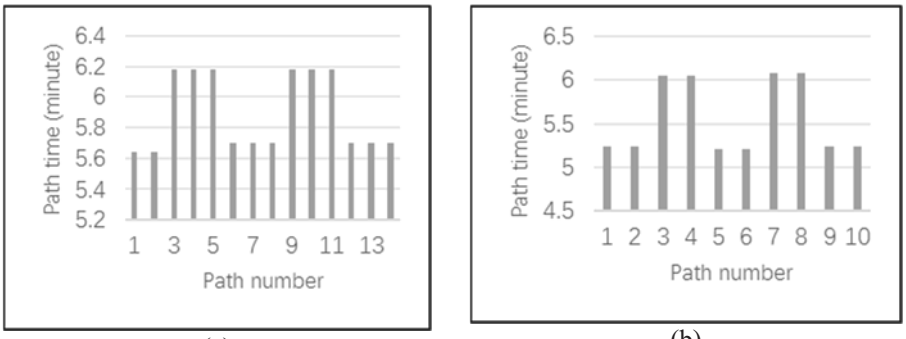

(a) (b)

Fig. 13 - The travel cost for each used path (OD:7-3).
(a) under initial signal timing. (b) under optimal signal timing

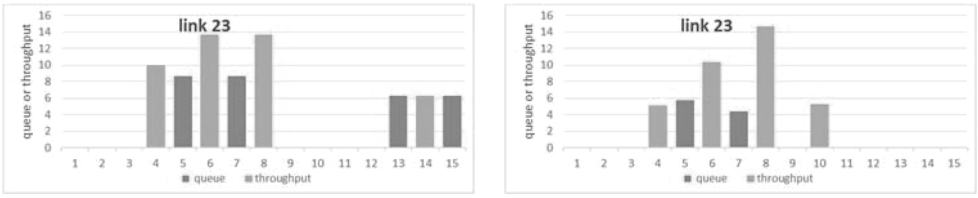

(a) (b)

Fig. 14 - The queued vehicles over red and throughput over the green at link 23 (abscissa is interval). (a) under initial signal timing. (b) under optimal signal timing

Tab. 1 - The flow on each used path and the travel cost for each used path under optimal signal timing for OD 1-9

No.	O	D	K	Path flow	Path time	Links on the path				Arrive time interval at each link on the path			
1	1	9	1	4.8949	5.2311	5	15	23	24	1	4	7	11
2	1	9	1	5.1051	5.231	3	4	9	19	1	4	7	11
3	1	9	2	4.4703	6.0668	5	13	17	24	2	5	8	12
4	1	9	2	5.5297	6.0669	3	7	14	19	2	5	8	12
5	1	9	3	5.2676	5.2121	5	15	23	24	3	6	9	13
6	1	9	3	4.7324	5.212	3	4	9	19	3	6	9	13
7	1	9	4	3.7978	6.0983	5	13	17	24	4	7	10	14
8	1	9	4	6.2022	6.0981	3	7	17	24	4	7	10	14
9	1	9	5	5.5438	5.2329	5	15	23	24	5	8	11	15
10	1	9	5	4.4562	5.2329	3	4	9	19	5	8	11	15

Randomly taking OD 1-9 as an example, the flow on each used path and the travel cost for each used path under optimal signal timing are shown in Table 1. Based on Table 1, we can see that there are 10 paths on the time-space network for OD 1-9. For OD 1-9, path "1-2" are for departure time interval 1, path "3-4" are for departure time interval 2, path "5-6" are for departure time interval 3, path "7-8" are for departure time interval 4, path "9-10" are for departure time interval 5, respectively. For time-dependent OD demand from OD 1-9 at time interval 2, it is divided into two branches with path flow being 4.4703 units and path time being 6.0668 minutes going along path "3", path flow being 5.5297 units and path time being 6.0669 minutes going along path "4". For path "3", 4.4703 units of vehicles first enter link 5 at time interval 2, then exit the link and enter link 13 at time interval 5, then exit link 7 and enter link 17 at time interval 8, then exit link 17 and enter link 24 at time interval 12, finally reach destination 9 after traversing link 24. The travel time for each of the 4.4703 units of vehicles is 6.0668 minutes. Since the path time of each path is equally 6.1815 minutes and the demand is 10, the overall travel cost for the demand is 60.668 minutes. The travel time for other demands can be analyzed similarly.

The queued vehicles over red time for some links are shown in Table 2, and the throughput over green time for some links are shown in Table 3.

Based on Table 2, randomly selecting link 2 as an example, we can see that for link 2, there are 5.5268 units of vehicles queued at the exit of it in time interval 5, and 6.2079 in time interval 7. The red color means the time interval is red time and the figure is the queue.

Based on Table 3, randomly selecting link 2 as an example, we can see that for link 2, there are 5.1058 units of vehicle leaving it in green interval 4, 10.2623 units of the vehicle in the green time interval 6, 15.5528 units of the vehicle in the green time interval 8, 5.3712 units of the vehicle in

the green time interval 10. The total vehicle throughput in green time increment is the sum of all vehicle throughput for all links and is computed as 665 units of vehicle. The green color means the time interval is green time and the figure is the throughput.

Under initial signal timing, the total vehicles queued at the red time increment is the sum of all queued vehicles for all links and is computed as 250. The overall queuing delay over red equals the number of queued vehicles in red time multiplied by red time which is 30 seconds in this example and the result is 125 minutes. The overall travel cost for all vehicles of all ODs is the product of the number of vehicles of all ODs and their travel cost and the result is 1176.4 minutes. Under optimal signal timing, the total vehicles queued at the red time increment is computed as 160. The overall queuing delay over red is 80 minutes. The overall travel cost for all vehicles of all ODs is 1033.6 minutes. We can see that both the overall queuing delay over red and the overall travel cost for all vehicles are decreased by optimizing signal timing at the DUORC status.

Tab. 2 - The queued vehicles at downstream of some links over red under optimal signal timing

Lin	interval k								
k	1	2	3	4	5	6	7	8	9
1	0	0	0	0	0	0	0	0	0
2	0	0	0	0	5.5268	0	6.2079	0	0
3	0	0	0	0	5.5268	0	6.2079	0	0
4	0	0	0	0	0	0	0	0	0
5	0	0	0	0	4.4732	0	3.7921	0	0
6	0	0	0	0	0	0	0	0	0
7	0	0	0	0	0	0	0	0	0
8	0	0	0	0	0	0	0	11.4901	0
9	0	0	0	0	4.4732	0	3.7921	0	0
10	0	0	0	0	0	0	0	0	0
11	0	0	0	0	0	0	0	5.5268	0
12	0	0	0	0	8.7282	0	9.3643	0	0
13	0	0	0	0	8.7282	0	9.3643	0	0
14	0	0	0	0	0	0	0	5.5268	0

Tab. 3 - The throughput at downstream of some links over green under optimal signal timing

Lin	interval k						
k	4	5	6	7	8	9	10
1	0	5.1058	0	4.7356	0	9.3449	0
2	5.1058	0	10.2623	0	15.5528	0	5.3712
3	5.1058	0	10.2623	0	15.5528	0	5.3712
4	0	5.1058	0	4.7356	0	9.3449	0
5	4.8942	0	9.7377	0	14.4469	0	4.7356
6	0	4.8939	0	5.3712	0	14.0240	0
7	0	11.0535	0	12.4158	0	0	0
8	0	0	0	0	0	11.4901	0
9	4.8942	0	9.7377	0	14.4469	0	4.7356
10	0	4.8939	0	5.3712	0	14.0240	0
11	0	4.2549	0	5.5722	0	5.5268	0
12	0	0	8.7282	0	9.3643	0	0
13	0	0	8.7282	0	9.3643	0	0
14	0	4.2549	0	5.5722	0	5.5268	0

The validity of the solution can be checked by some examples as follows.

Path flow conservation constraint:

$f_2^{19} = f_{1,2}^{19} + f_{2,2}^{19} + f_{3,2}^{19}$ =5.7430+1.3346+2.9224=10

Link inflow conservation constraint:

$u_{8,9}^{91} + u_{8,9}^{73}$=3.8016+3.0317+3.8016+3.0317=13.6667=u_9^8

Link outflow conservation constraint: $v_{8,13}^{91} + v_{8,13}^{73} = 13.6667 = v_8^{13}$.

Node flow conservation constraint: $\sum_{a\in B(6)} v_{a,8}^{rs} = \sum_{a\in B(6)} v_a^8 = v_9^8 + v_{14}^8 + v_{20}^8 =$ 6.3331+0+6.3334=12.6665.

$\sum_{a\in A(6)} u_{a,8}^{rs} = \sum_{a\in A(6)} u_a^8 = u_{10}^8 + u_{12}^8 + u_{19}^8$ = 6.3331+0+6.3334=13.6665.

Link flow propagation constraint: $u_{8,9}^{91} = v_8^{91}[9 + \bar{\tau}_8^9] = v_{8,13}^{91}$ = 6.8333, $u_{8,9}^{73} = v_8^{73}[9 + \bar{\tau}_8^9] = v_{8,13}^{73}$ =6.8333, where τ_8^9 = 1.7568 minutes.

For a time increment of 30 seconds, $\bar{\tau}_8^{10} = 4$.

Inflow and queue equation: $u_2^4 = q_{2,7}^r$ = 8.6654, for link 2, time 7 ∈ red. $u_2^5 = q_{2,8}^g$ =5.0005, for link 2, time 8 ∈ $green$.

Outflow and queue equation: $v_2^7 = 0$, for link 2, time 7 ∈ red, $v_2^8 = q_{2,7}^r + q_{2,8}^g = q_2^8$ = 13.6669, for link 2, time 8 ∈ $green$.

The actual travel cost on the used paths of OD 1-9 departing at increment 1 is as follows:

$c_{1,1}^{19} = \tau_3^1 + \tau_7^4 + \tau_{17}^7 + \tau_{24}^{11}$ = 1.2416+1.2832+1.7416+1.3749= 5.6412 minutes.

Similarly, $c_{1,1}^{19}$ =5.6412 minutes.

All these meet the conditions of the DUORC problem. This shows the validity of the model and algorithm.

5. Conclusions

Selecting the length of the increment is important in solving the optimal signal timing (OST) and the dynamic user optimal route choice (DUORC) problem. In this paper, the OST and the DUORC problem was studied with the consideration of assignment increment. The problem is modeled as a three-level problem. The first level is setting the increment. The second and the third level are a non-cooperative Stackelberg game. The result of the experimental study indicates that a reasonable increment should be used in solving the OST-DUORC problem. Concretely speaking, a smaller increment is preferred in solving the OST-DUORC problem as long as the minimum green time is reached. The increment equalling the length of the minimum green time can be the reference in practice.

Furthermore, this paper presents a conception of a new OST-DUORC travel guidance system, including the framework of the system and the algorithm for it. Based on the result of the experimental study and the method, the traffic center of a city selects an appropriate increment (as small as possible as long as the minimum green time is reached) in solving the OST-DUORC problem on the work station (a huge computer) of the traffic center, and then finds the OST for intersections and the optimal routes for travelers by running the second and third level model. The information on the optimal routes will be sent to the on-board devices on the vehicles of the travelers and shown on the electronic map. The information on the optimal signal timing will be sent to traffic control centers or signal timing devices at intersections and optimal signal timing will be set for intersections. All the information will be sent through the communication system.

The new OST-DUORC travel guidance system can provide the links/streets and nodes/intersection and the signal timing at each intersection and the traversing time on each street on the route. Meanwhile, the overall queuing delay of all vehicles at intersections is minimal and the route choice of all travelers is in DUO status. Future study may consider the optimal departure time in addition to the optimal route choice and optimal signal timing.

References

1. Abdelfatah, A. S.; Mahmassani, H. S. (1998) System Optimal Time-Dependent Path Assignment and Signal Timing in Traffic Network, TRR 1645, pp. 185–93.
2. Abdelfatah, A. S.; Mahmassani, H. S. (2001) A simulation-based signal optimization algorithm within a dynamic traffic assignment framework, in Proceedings of 2001 IEEE Intelligent Transportation Systems

Conference, Oakland, CA, pp. 428–33.
3. Karoonsoontawong, Ampol; Waller, S., Travis. (2009) Application of Reactive Tabu Search for Combined Dynamic User Equilibrium and Traffic Signal Optimization Problem. Transportation Research Record: Journal of the Transportation Research Board 2090, pp. 29–41. DOI: 10.3141/2090-04.
4. Sun, D.; Benekohal, R. F.; Waller, S. T. (2006) Bi-level Programming Formulation and Heuristic Solution Approach for Dynamic Traffic Signal Optimization. Computer-Aided Civil and Infrastructure Engineering, 21: 321–333.
5. Waller, S. T. (2000) Optimization and Control of Stochastic Dynamic Transportation Systems: Formulations, Solution Methodologies, and Computational Experience. PhD thesis. Northwestern University, Evanston, Ill., 2000.
6. Beard, C.; Ziliaskopoulos, A. (2006) System Optimal Signal Optimization Formulation. In Transportation Research Record: Journal of the Transportation Research Board 1978, pp. 102–112.
7. Varia, H. R.; Dhingra, S. L. (2004) Dynamic optimal traffic assignment and signal time optimization using genetic algorithms. Computer-Aided Civil and Infrastructure Engineering 19, 260–273.
8. Xu, Tianze; Ran, Bin; Cui, Yingying. (2023) Dynamic user optimal route choice problem on a signalized transportation network, Transportation Engineering, 13, 100153.
9. https://doi.org/10.1016/j.treng.2022.100153.
10. Smith, M. J.; Wisten, M. B. (1995) A continuous day-to-day traffic assignment model and the existence of a continuous dynamic user equilibrium. Annals of Operations Research 60, 59–79.
11. Sheffi, Y. (1985) Urban Transportation Networks. Prentice-Hall, INC, Englewood Cliffs, New Jersey.
12. Gartner, N. H.; Al-Malik, M. (1996) Combined Model for Signal Control and Choice in Urban Networks, TRR 1554, pp. 27–35.
13. Gartner, N. H.; Stamatiadis, C. (1997) Integration of Dynamic Assignment with Real-Time Traffic Adaptive Control, TRR 1644, pp. 150–56.
14. Smith, M. J. (1979) The existence, uniqueness and stability of traffic equilibrium, Transportation Research, 13B, 235–304.
15. Smith, M. J. (1980) A local traffic control policy which maximizes the overall travel capacity of an urban road network, Traffic Engineering and Control, 21, 298–302.
16. Smith, M. J. (1981a) The existence of an equilibrium solution to the traffic assignment problem when there are junction intersections, Transportation Research, 15B, 443–51.
17. Smith, M. J. (1981b) Properties of a traffic control policy which ensure the existence of traffic equilibrium consistent with the policy, Transportation Research, 15B, 453–62.
18. Smith, M. J.; Van Vuren, T.; Heydecher, B. G.; Vilet, D. V. (1987) The interaction between signal control policies and route choice, Paper Presented at the 10th International Symposium on Transportation and Traffic Theory, Cambridge, MA, pp. 319–38.
19. Sun, D. (2005) A Bi-Level Programming Formulation and Heuristic Solution Approach for Traffic Control Optimization in Networks With Dynamic Demand and Stochastic Route Choice. Traffic Signal Controllers (2005).
20. Sun, D.; Benekohal, R. F.; Waller, S. T. (2006) Bi-level Programming Formulation and Heuristic Solution Approach for Dynamic Traffic Signal Optimization. Computer-Aided Civil and Infrastructure Engineering 21, 321–333.
21. Chen, O. J.; Ben-Akiva, M. E. (1998) Game-theoretic formulations of the interactions between dynamic traffic control and dynamic traffic assignment, Transportation Research Record, 1617, 179–88.
22. Ren, Gang; Zhou, Pingshan; Gao Jinyao. (2020) Optimization of Dynamic Traffic Allocation and Signal Control under Auto-Driving Mode. 20th COTA International Conference of Transportation Professionals. CICTP 2020: Transportation Evolution Impacting Future Mobility (100–112).
23. Zeng, Ying; Ma, Yingying. (2018) A Bi-Level Model of Dynamic Lane-Use and Traffic Signal for Intersections. CICTP 2018: Intelligence, Connectivity, and Mobility (2626–2638)
24. Fang; Clara, Fang. (2014) Traffic Signal Optimization and Simulation Using Fuzzy Dynamic Programming. CICTP 2014: Safe, Smart, and Sustainable Multimodal Transportation Systems (2140–2151).
25. Wang, Qinzheng; Yang, Xianfeng; Yuan, Yun. (2021) Dynamic Multipath Signal Progression Control

Based on Connected Vehicle Technology. Journal of Transportation Engineering, Part A: Systems. 147(10).
26. Yuan, Yun; Liu, Yue; Liu, Weiyan. (2019) Dynamic Lane-Based Signal Merge Control for Freeway Work Zone Operations. Journal of Transportation Engineering, Part A: Systems. 145(12).
27. Gao, Yunfeng; Liu, Yue; Hu, Hua; Ye, Y. E. (2019) Intersection Dilemma-Zone Protection as a Dynamic Signal-Optimization Problem with Model Predictive Control. Journal of Transportation Engineering, Part A: Systems. 145(11).
28. Yang, Xiaoyu; Park, JeeWoong; and Cho, Yong K. Adaptive Signal-Processing for BLE Sensors for Dynamic Construction Proximity Safety Applications. Construction Research Congress 2018: Safety and Disaster Management (84-93).
29. Di Gangi, Massimo; Cantarella, Giulio E.; Di Pace, Roberta; Memolib, Silvio. (2016) Network traffic control based on a mesoscopic dynamic flow model. Transportation Research Part C: Emerging Technologies. 66: 3-26.
30. https://doi.org/10.1016/j.trc.2015.10.002
31. Yao, Z.; Shen, L.; Liu, R.; Jiang, Y.; Yang, X. (2020) A Dynamic Predictive Traffic Signal Control Framework in a Cross-Sectional Vehicle Infrastructure Integration Environment, in IEEE Transactions on Intelligent Transportation Systems, 21(4): 1455-1466. doi: 10.1109/TITS.2019.2909390.
32. Yao, Zhihong; Jiang, Yangsheng; Zhao, Bin; Luo, Xiaoling; Peng, Bo. (2020) A dynamic optimization method for adaptive signal control in a connected vehicle environment. Journal of Intelligent Transportation Systems. 24(2): 184-200.
33. doi:10.1080/15472450.2019.1643723
34. Wang, Pangwei; Cheng, Jun; Ni, Haoyuan; Li, Yinghong. (2018) Research on Traffic Signal Dynamic Optimization Model for Urban Intersections Based on Connected Vehicles. CICTP 2018: Intelligence, Connectivity, and Mobility (245–255)
35. Zhang, Huilin; Cheng, Lin; Tu, Qiang; Wang, Qiaozhen. (2017) Research on Dynamic Nature of Dilemma Zone at Signalized Intersections. CICTP 2017: Transportation Reform and Change—Equity, Inclusiveness, Sharing, and Innovation (4258–4266)
36. Li, Xu; Wang, Hao; Chen, Jun. (2013) Dynamic Lane-Use Assignment Model at Signalized Intersections under Tidal Flow. Fourth International Conference on Transportation Engineering. ICTE 2013 (2673–2678)
37. Mintsis, Evangelos; Vlahogianni, Eleni I.; Mitsakis, Evangelos. (2020) Dynamic Eco-Driving near Signalized Intersections: Systematic Review and Future Research Directions. Journal of Transportation Engineering, Part A: Systems. 146(4).
38. Wu, Xia; Zhao, Xiangmo; Xin, Qi; Yu, Shaowei. (2018) Dynamic Speed Optimization in the Vicinity of Signalized Intersections during Green Phase. CICTP 2018: Intelligence, Connectivity, and Mobility (2318–2329)
39. Guo, Mengdi; Wang, Dingyuan; Fu, Daocheng; Yan, Haoyang. (2019) Dynamic Estimation of Queue Length at Signalized Intersections Using GPS Trajectory Data. CICTP 2019: Transportation in China—Connecting the World (2660 - 2671)
40. Krause, Cory; Kronpraset, Nopadon; Bared, Joe; Zhang, Wei. (2015) Operational Advantages of Dynamic Reversible Left-Lane Control of Existing Signalized Diamond Interchanges. Journal of Transportation Engineering. 141(5).
41. Liang, Shidong; Chen, Lijuan; Wang, Ying; Han, Yilei. (2022) Optimization Design and Evaluation Analysis of Dynamic Straight-Right Lane at Signalized Intersection. Journal of Highway and Transportation Research and Development (English Edition). 16(1): 82–91.
42. Zhang, Lin; Wu, Weiming; Huang, Xuanwei. (2016) A Dynamic Optimization Model for Adjacent Signalized Intersection Control Systems Based on the Stratified Sequencing Method. Journal of Highway and Transportation Research and Development (English Edition). 10(1): 85–91.
43. Macioszek, Elżbieta; Iwanowicz, Damian. (2021) A Back-of-Queue Model of a Signal-Controlled Intersection Approach Developed Based on Analysis of Vehicle Driver Behavior. Energies ISSN: 1996-1073. 14(4): 1204. doi: 10.3390/en14041204
44. Chen, P.; Liu, H.; Qi, H.; Wang, F. (2013) Analysis of delay variability at isolated signalized intersections.

J. Zhejiang Univ. 2013, 14, 691–704.
45. Viti, F.; Van Zuylen, H. J. (2019) Markov mesoscopic simulation model of overflow queues at multilane signalized intersections. Adv. OR AI Methods Transp. 2005, 475–481. Available online: http://www.iasi.cnr.it/ewgt/16conference/ID87.pdf
46. Gasz, K. (2004) Zastosowanie szeregów czasowych do opisu długo´sci kolejek na wlotach skrzyzowa ´n. In Proceedings of the 50. ˙Jubileuszowa Konferencja Naukowa Komitetu Inzynierii L ˛adowej i Wodnej PAN i Komitetu Nauki PZITB "Krynica 2004", ˙ Krynica, Poland, 12–17 September 2004.
47. Shou, Y.; Xu, J. (2010) Multi-objective optimization of oversaturated signalized intersection based on fuzzy logic. In Proceedings of the 8th World Congress on Intelligent Control and Automation, Jinan, China, 6–9 July 2010.
48. Kafash, M.; Sharif, M. J.; Menhaj, M. B.; Maleki, A. (2013) Designing fuzzy controller for traffic lights to reduce the length of queues in according to minimize extension of green light time and reduce waiting time. In Proceedings of the 13th Iranian Conference on Fuzzy Systems (IFSC), Qazvin, Iran, 27–29 August 2013; pp. 1–6.
49. Mucsi, K.; Khan, A. M.; Ahmadi, M. (2011) An adaptive neuro-fuzzy inference system for estimating the number of vehicles for queue management at signalized intersections. Trans. Res. Part C 2011, 19, 1033–1047.
50. Van Zuylen, H. J.; Viti, F. (2003) Uncertainty and the dynamics of queues at controlled intersections. IFAC Proc. 2003, 36, 43–48.
51. Viti, F.; Van Zuylen, H. J. (2009) The dynamics and the uncertainty of queues at fixed and actuated controls: A probabilistic approach. J. Intell. Transp. Syst. Technol. Plan. Oper. 2009, 13, 39–51.
52. Cao, J.; Hu, D.; Hadiuzzaman, M.; Wang, X.; Qiu, T.Z. (2014) Comparison of queue estimation accuracy by shockwave-based and input-output-based models. In Proceedings of the 17th International IEEE Conference on Intelligent Transportation Systems (ITSC), Qingdao, China, 8–11 October 2014; pp. 2687–2692.
53. Ng, K. M.; Reaz, M. I. (2015) A Comparative Study of the LWR-IM Traffic Model and Shockwave Analysis. In Proceedings of the 2015 IEEE Conference on Systems, Process and Control (ICSPC 2015), Bandar Sunway, Malaysia, 18–20; pp. 39–43.
54. Srivastawa, A.; Jin, W. L.; Lebacque, J. P. (2015) A modified Cell Transmission Model with realistic queue discharge features at signalized intersections. Transp. Res. Part B Methodol. 2015, 81, 302–315.
55. Nie, X. J.; Zhang, H. M. (2005) The Delay-Function-Based Link Models: their properties and computational issues. Transportation Research Part B, 39, 729-751.

Advances in Transportation Studies: an international Journal 66 (2025)

ISBN 979-12-218-1935-9 – ISSN 1824-5463 – DOI 10.53136/97912218193592 – pag. 19-38

Vision transformer for detecting traffic congestion using image mapping

A. Khalfi[1] M. Guerroumi[1] T. Haid[2] N. Laradji[2]

[1]*Faculty of Computer Science, Artificial Intelligence and Data Science Department, University of Science and Technology Houari Boumediene, Algiers, Algeria.*
[2]*Matter Sciences and Computer Science Faculty, Department of Computer Science, University of Djilali Bounaama, Khemis Miliana, Algeria.*
email: a.khalfi@univ-dbkm.dz

subm. 11st August 2024 *approv. after rev. 29th November 2024*

Abstract

Leveraging advanced computer vision techniques, we present a novel method for analyzing and categorizing traffic videos by utilizing an image mapping technique combined with a UniVit (Unit Vision Transformer) model. First, video data is transformed into an image dataset, where each frame undergoes a mapping process based on vehicle detection using the YOLOv8s algorithm. These mapped images are then input into a vision transformer, which utilizes attention mechanisms to identify and analyze complex patterns across frames. The approach is evaluated on the UCSD (University of California San Diego) dataset, which features diverse weather conditions such as clear, overcast, and rainy scenarios, enabling a rigorous assessment under varied environments. Our method achieves a notable accuracy score of 99.89%, surpassing previous approaches on the UCSD benchmark. This improvement underscores the effectiveness of combining image mapping with advanced vision transformers, suggesting promising applications for intelligent traffic management systems aimed at mitigating traffic issues.

Keywords – vision transformer, traffic congestion, YOLOv8s, image mapping

1. Introduction

The rapid influx of people to cities strains traffic systems, causing economic hardship and disrupting vital urban services like healthcare and public safety [1]. According to Bashingi et al. [2], poor traffic management leads most noticeably to serious issues like longer commutes, but the impact likely extends beyond mere inconvenience. Traffic congestion doesn't just affect cities – it takes a toll on individuals too. Throughout peak traffic periods, wasted time, neurocognitive weariness and elevated airborne impurities. 2030 is expected to see traffic congestion costs across France, Germany, the United Kingdom, and the United States rise to 55 billion US dollars [3]. A country's advancement hinges on both fostering economic development and ensuring the convenience of its road users, a task unattainable without streamlined traffic movement. The capability to anticipate traffic congestion provides officials and commuters with the essential lead time to allocate resources effectively, ensuring seamless travel experiences for all. Therefore, there is a pressing need for a universal and versatile traffic congestion detection system [4]. Intelligent transportation systems (ITS) offer cutting-edge solutions for traffic management. Camera networks, a recent advancement in ITS, are proving particularly promising. In contrast to traditional loop

detectors, video-based systems are less intrusive to install, more cost-effective, and provide a richer grasp of traffic circulation trends. Deep learning tackles massive datasets from cameras to reveal intricate traffic patterns and congestion hotspots, Chakraborty et al. [5] proposed two distinct deep learning methodologies were employed: You Only Look Once (YOLO) and Deep Convolutional Neural Network (DCNN), to identify instances of traffic congestion within camera footage. However, these methods depend heavily on data quality and quantity. Traditional traffic data often falls short. Saini and Susan [6] found that deep learning thrives on richer datasets, while smaller ones lead to subpar performance. Data augmentation, a technique that creates variations of existing data, bridges the gap between training and testing data, as shown by Shorten and Khoshgoftaar [7]. Advanced image processing algorithms and object detection methods have created new opportunities for vision-based smart traffic control systems [8]. Vision Transformers (ViTs) have demonstrated success in various image recognition tasks, but their application to traffic classification remains underexplored. This motivated us to investigate their potential in this domain. While Ramana et al. [9] investigated the use of both CNNs and ViTs for urban traffic flow prediction, this study employed the You Only Look Once (YOLOv8s) detector to identify automobiles in the image, followed by the application of Vision Transformers (ViTs) for traffic congestion classification. Drawing on the advancements in accuracy demonstrated by the YOLOv8s algorithm as highlighted by Lou et al. [10], This streamlines our method and increases its potential applicability for real-time use. The main contributions of this research cover the following points:

1. We apply the Region of Interest (ROI) technique to downscale the image and then resize it further to a more compact format, achieving high classification accuracy while minimizing memory usage.
2. The image mapping stage involves simplifying the dataset, which in turn reduces computation time and task complexity.
3. We employ a Unit Vision Transformer (UniViT) consisting of a single head layer to classify traffic congestion, facilitated by the prior implementation of image mapping using YOLOv8s, which streamlines the classification process.
4. We assess the proposed method under various weather conditions by using the publicly available UCSD dataset [11] highlight its superiority compared to current methods.

The remainder of the paper is organized as follows: Section 2 provides the literature review. Section 3 elaborates on the proposed method, covering various stages. Section 4 discusses the experimental results and benchmarks the proposed method against other recent techniques. Finally, the paper concludes with section 5.

2. Literature review

Video cameras have become integral in traffic congestion estimation due to their non-intrusive installation on road infrastructure. Analyzing traffic videos generally requires two key elements: vehicle density and speed. Various studies have explored methods to estimate these factors effectively.

Zhao et al. [12] propose a new solution for automatic traffic congestion detection traffic congestion using Remote Transportation Microwave Sensors (RTMS) installed on Chinese highways. This approach uses pattern matching and correlation analysis to detect congestion and introduces virtual nodes for improved accuracy, achieving notable results on the Beijing-Harbin highway. However, RTMS sensors depend on sufficient data density, which may not be feasible in sparse sensor installations. Hu et al. [13] design new method to improve the efficiency of traffic